

# TXRF spectrometry in the bioanalytical sciences: A brief review

Ramón Fernández-Ruiz, Doctor in Science 

Servicio Interdepartamental de Investigación (SIdI). Laboratorio de TXRF, Universidad Autónoma de Madrid (UAM), Madrid, Spain

## Correspondence

Ramón Fernández-Ruiz, Servicio Interdepartamental de Investigación (SIdI). Laboratorio de TXRF, Universidad Autónoma de Madrid (UAM), Cantoblanco 28049, Madrid, Spain. Email: ramon.fernandez@uam.es

## Funding information

Universidad Autónoma de Madrid

This work describes the basic principles of Total-reflection X-Ray Fluorescence (TXRF) spectrometry and some of its most outstanding applications for investigating metal traces, mainly in biological and biomedical samples. TXRF is an analytical technique that combines the versatility of elemental analysis by X-ray energy dispersion with a low detection limit in the order of picograms of absolute mass or a few ppb ( $\mu\text{g L}^{-1}$ ) as concentration. The microanalytical capacity of TXRF allows the study of small sample quantities. The TXRF can perform qualitative and mass ratio analyses of the elements present in a sample of only a few hundred nanograms. These properties are of great importance in the research of metal traces in biological systems, as they allow fast, precise, and accurate characterisation of the elemental fingerprint at trace level. Its successful application in studies of the coordination kinetics of new platinum-based antitumor drugs with DNA, its application in the study profile of the metal in healthy and cancerous human tissues, or even its application in the study of the processes of metal diffusion through cell membranes are just a few examples of TXRF capabilities in the biomedical sciences. This brief review's main objective is to provide an overview of the physical principles and possibilities of TXRF spectrometry. It also highlights some of the most outstanding applications that have been developed so far, mainly in the biological field, so that the reader can evaluate their potential applications.

## 1 | INTRODUCTION

Total-reflection X-Ray fluorescence (TXRF) is an X-ray spectrometric technique derived from classical energy dispersive X-ray fluorescence (EDXRF). This fact could be the reason why sometimes both techniques are confused, and therefore they are erroneously considered to be equivalent. The Source-Sample-Detector system's geometric variation, which distinguishes TXRF from conventional EDXRF, has very positive consequences in physical and analytical aspects that differentiate it from

the most traditional X-ray spectrometric techniques. Working in the condition of total reflection implies the generation of a field of X-ray Standing Waves (XSW) on the surface of the sample-carrier, which is the reason for the unique properties of the TXRF technique. The unique monographic book on TXRF has been recently updated to the second edition by Reinhold Klockenkämper and Alex Von Bohlen.<sup>[1]</sup> Nowadays, this book represents the essential pillar to begin the way to learn and practice the TXRF spectrometry of beginners and experts scientist. The TXRF is an analytical tool that can be used to

This is an open access article under the terms of the Creative Commons Attribution-NonCommercial License, which permits use, distribution and reproduction in any medium, provided the original work is properly cited and is not used for commercial purposes.

© 2021 The Author. *X-Ray Spectrometry* published by John Wiley & Sons Ltd.

analyse small sample quantities. Thus, a few micrograms of the sample can be evaluated in a relatively simple way being the analysed mass sample in the order of hundreds of nanograms deposited over the reflector surface. TXRF microanalytical capability is a powerful tool in analysing biosamples since these type of samples are usually available in small quantities. On the other hand, recently has been approved for the period 2019–2023 the CA-18130 European COST Action, named ENFORCE-TXRF, with the primary finality of improving the knowledge and the analytical potentiality of the TXRF spectrometry at the industry, research and education. In this way, renewed efforts are being applied at an international level to explore and develop the analytical capabilities of TXRF spectrometry in all scientific fields in general but in the bioanalytical in particular.<sup>[2]</sup>

This small review has the main objective of briefly introducing TXRF physical principles and their analytical advantages and limitations with a better criterion. The second goal is to show only a partial summary of the most outstanding applications developed in bioanalysis using TXRF spectrometry.

## 1.1 | Historical background

In 1923, Compton discovered the phenomenon of total reflection X-ray<sup>[3]</sup> showed that the X-ray reflectivity of a flat material increases below a specific angle which depends on the material that it is made the reflector which acts as sample support and the energy of the incident X-ray. This angle is well-known by the TXRF community as the critical angle. In the typical case of Mo K $\alpha$  source and quartz as a reflector, a critical angle around 0.1° is a good estimation. It was not until 1971, almost 50 years later, when Yoneda and Horiuchi<sup>[4]</sup> had the idea of generating the excitation-emission X-ray fluorescence of the atoms deposited over a reflector in total reflection geometry (Figure 1). In this way, the total reflection effect was used to induce an amplified excitation region due to the double excitation of the sample presents over the reflector, that is, by the incident and totally reflected beam. This idea materialised in a few but innovative works during the 70s and early 80s.<sup>[5–7]</sup>

These studies assumed the formal appearance of the TXRF in the field of X-ray spectrometry. The TXRF technique's appearance allowed that the X-ray spectrometry, relegated since the decade of the 60s mainly to the analysis of major elements, could be reintroduced with more success in the field of atomic chemical analysis at trace and ultra-trace levels. However, this development occurred about a century after Bunsen and Kirchhoff's groundbreaking research regarding the use of flame

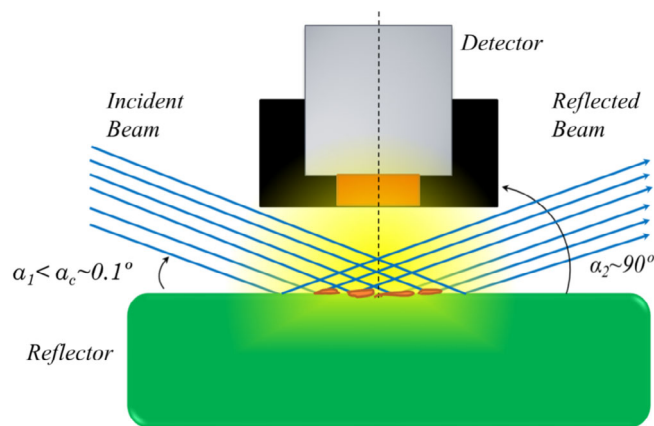


**FIGURE 1** Basic diagram of total-reflection X-Ray fluorescence geometry

techniques for spectroscopic analysis. This period allows the flame techniques continuous technological development and instrumental improvement, cost minimisation, standardisation, and routine incorporation in the great majority of the world's analytical laboratories. This long period also has generated a significative analytical bibliographic background related to flame techniques. Thus, the intellectual challenge poses the researcher to break with 100 years of scientific bibliography, have caused that the incorporation of the TXRF has been slow and, even today, little known and not widespread enough for the biological, biomedical and much other scientific fields. Flame techniques have covered all analytical ranges during this long period, micro (0.01%–1%), trace (0.1–100 ppm, mg/kg) and ultra-trace (less than 100 ppb,  $\mu\text{g/kg}$ ). Moreover, the continuous improvement of the ICP-MS technique, particularly with the development of the multiple collision cells to minimise interfering species, converts into an excellent analytical method. The main drawback of all flame techniques is their use of high purity gases, which imply an elevated cost of service and maintaining.

In the case of the TXRF, the major drawback was the high cost of the first generations of laboratory instruments. Today, the price is being reduced due to the emergence of new generation technologies as X-ray micro-sources with high-flux, polycapillary X-ray optics or Silicon Drift Detectors (SDD) with high counting rate and resolution. These improvements have allowed the progressive minimisation of costs of the TXRF instrumentation.<sup>[8]</sup> Nowadays, the TXRF instrument costs are competitive with conventional Atomic-Absorption (AAS) or ICPS instruments. This fact opens the door to the TXRF to all scientific and industrial fields where the metal traces analysis would necessary. The enormous difference in use and maintenance costs between TXRF

and flame/plasma instruments also opens another door. In this analytical facet, TXRF is a clear winner because it only needs a low power electric connection, next to the usual material in an analytical laboratory, to obtain high-quality results at ppb ( $\mu\text{g L}^{-1}$ ) detection levels.

In parallel, TXRF spectrometry has been able to mature mainly due to the celebration of biennial monographic conferences on TXRF and related methods. The TXRF international conferences held so far have been the following: 1986 in Geesthacht (Germany), 1988 in Dortmund (Germany), 1990 Vienna (Austria), 1992 in Geesthacht (Germany), 1994 in Tsukuba (Japan), 1996 in Dortmund (Germany), and Eindhoven (Netherlands), 1998 in Austin, Texas (USA), 2000 in Vienna (Austria), 2002 in Madeira (Portugal), 2003 in Awaji Island, Hyogo (Japan), 2005 in Budapest (Hungary), 2007 Trento (Italy), 2009 in Goteborg (Sweden), 2011 in Dortmund (Germany), 2013 in Osaka (Japan), 2015 in Denver (USA), 2017 in Brescia (Italy), and finally 2019 in Girona (Spain).

To date, TXRF has been applied successfully to solve many problems in inherently difficult materials and many scientific fields such as medicine,<sup>[9]</sup> environmental sciences,<sup>[10]</sup> archaeology,<sup>[11]</sup> physics of materials,<sup>[12]</sup> electronics,<sup>[13]</sup> art,<sup>[14]</sup> nanotechnology<sup>[15]</sup> or biology,<sup>[16]</sup> among many others. However, a long way remains to be done within the scope of its potential applications. As Figure 2 shows, since Yoneda and Horiuchi's pioneering article in 1971,<sup>[4]</sup> the number of scientific publications related to TXRF or their applications were practically null until 1985. It was from this year when the first TXRF instruments were commercialised by Rich & Seifert in Germany. From this time, the new TXRF analytical

technology began to be each time more known recognised by the international scientific community.

The database of technical literature is at present approximately 1900 international scientific publications. This value indicates that there are still many scientific fields where TXRF can demonstrate its potential. Figure 2 also shows the annual number of scientific publications recorded in the same period. The yearly scientific productivity was increased with a positive slope from 1985 to 2000, being stable since that year with a value of around 70 international publications per year. Periodic biannual increases are also visible in Figure 2. This periodicity is because coincides with the years after the celebration of the international TXRF conferences. Consequently, scientific contributions presented at these conferences have been usually compiled and published in special issues of the journal *Spectrochimica Acta Part B: Atomic Spectroscopy*. Today, these are the more essential and extended technical literature<sup>[17]</sup> alongside the excellent TXRF monograph published by Reinhold Klockenkämper and Alex von Bohlen.<sup>[1]</sup>

## 1.2 | Physical background

An X-ray beam follows a linear path through a homogeneous medium. However, like visible light, if the X-ray beam finds a new medium along its path, this will vary from the original. In this way, part of the incident X-ray beam will be reflected towards the first medium, and the rest will be refracted towards the second (Figure 3). The angle of incidence  $\alpha_1$  and the refracted angle  $\alpha_2$  follow Snell law

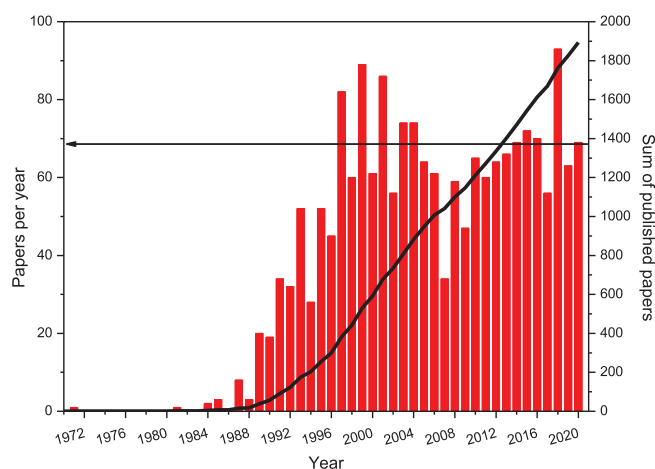


**FIGURE 2** The number of papers published by year (bars) and its accumulated sum (line), where “TXRF” has been used as keywords in SciFinder® 2020

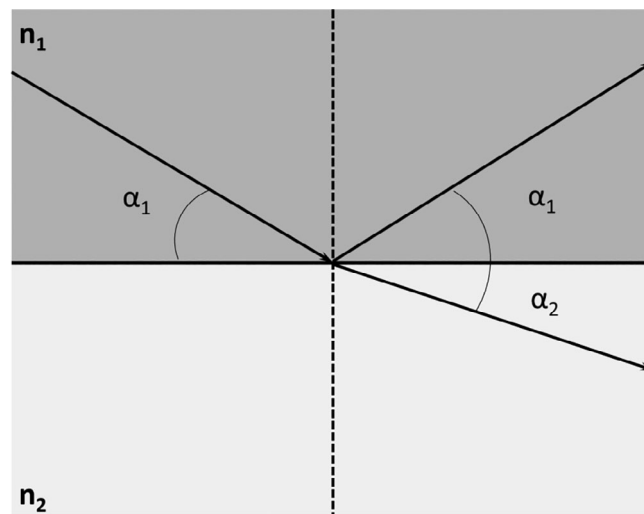


**FIGURE 3** Reflection and refraction of an X-ray beam crossing two medium with refractive index  $n_2 < n_1$

$$n_1 \cos \alpha_1 = n_2 \cos \alpha_2, \quad (1)$$

where  $n_1$  and  $n_2$  are the refractive indices of media 1 and 2, respectively. For the X-rays, any medium is optically less dense than vacuum and any solid optically less dense than air, that is,  $n_{\text{solid}} < n_{\text{air}} \approx 1$ . If the angle  $\alpha_2$  is zero, the refracted beam will emerge tangentially to the interface. Therefore, there must be a critical angle for the incident beam,  $\alpha_1 = \alpha_c$ , where the refracted beam acquires an angle  $\alpha_2 = 0$ .

According to Snell law and considering that  $n_{\text{air}} \sim 1$

$$\cos \alpha_c = n_{\text{solid}}. \quad (2)$$

Moreover, the refractive index of the solid reflector has the complex form

$$n_{\text{solid}} = 1 - \delta - i\beta, \quad (3)$$

where  $i$  is the imaginary unit and the parameters  $\delta$  and  $\beta$  are the scattering and absorption parameters of the material respectively. From Equations (2) and (3) we can estimate the value of the critical angle of any material in the form

$$\alpha_c \approx \sqrt{2\delta} \approx \frac{1.65}{E} \sqrt{\frac{Z_m}{A_m}} \rho, \quad (4)$$

where  $E$  is the incident photon energy (keV),  $Z_m$  is the atomic number,  $A_m$  is the atomic weight (g/mol), and  $\rho$  the density of the material (g/cm<sup>3</sup>).<sup>[18]</sup>

For incidence angle lower than  $\alpha_c$ , Snell law does not give real values for refraction angle  $\alpha_2$ . In this case, the X-ray beam only penetrates some nanometers in the second medium, and the interface behaves like a mirror close to the ideal, fully reflecting the incident beam to the first medium. Thus, for angles below the critical angle, the incident beam interferes constructively with the

reflected beam, generating a field of XSW, as Figure 4 shown.

The phenomenon of constructive interference generated in the XSW field implies that the intensity inside the interference region is amplified. On average, the amplification is around twice than of conventional XRF. If there is a sample deposited into the XSW region, this will also be excited twice. Another way of understanding this amplification effect is considering that the atoms are excited by both the incident and the totally reflected beam. The stationary wave field's cross-section has a triangular shape, and I like to call it a “magic triangle”. Bedzyk et al.<sup>[19]</sup> deduced in 1989 a general equation for the distribution of intensity,  $I(\alpha, z)$  into the XSW field in terms of their angular dependence  $\alpha$  and its position  $z$  above the reflector. Equation (5) gives the shape of this intensity distribution

$$I(\alpha, z) = I_0 \left[ 1 + R(\alpha) + 2\sqrt{R(\alpha)} \cos \left( \frac{2\pi z}{\lambda_{\text{XSW}}} - \phi(\alpha) \right) \right], \quad (5)$$

where  $I_0$  is the intensity of the primary beam, the argument of cosine is the phase difference between incident and reflected waves, broken down into two components, a spatial  $2\pi z/\lambda_{\text{XSW}}$  and a phase shift  $\phi(\alpha)$ . Finally,  $R(\alpha)$  is the reflectivity of the material used as a reflector, or sample carrier, for each angle of incidence  $\alpha$ .

If a sample is introduced within the XSW field, the atoms will be excited, and the fluorescence emissions intensity will be proportional to the intensity of the XSW field. Now assuming that the contribution to the spectral background of the sample carrier is infinitely thick, optically flat and homogeneous, the intensity of the evanescent wave field that penetrates the reflector is given by the equation

$$I(\alpha, z) = I_0 \left[ 1 + R(\alpha) + 2\sqrt{R(\alpha)} \cos(\phi(\alpha)) \right] \exp \left( -\frac{z}{z_e} \right), \quad (6)$$

where the new parameter  $z_e$ , or depth of penetration, is defined as the depth that X-ray beam penetrates in the medium such as its intensity is reduced by a factor  $1/e$ . Note that the evanescent wave's penetration is only of few nanometers and remains practically constant for angles below the critical angle in total reflection condition. Figure 5 shows the intensity signal of fluorescence associated with a sample of Fe deposited with a typical thickness of 500 nm on a Si reflector next to the Si reflector's fluorescence signal with respect to the angle of incidence of the primary beam.

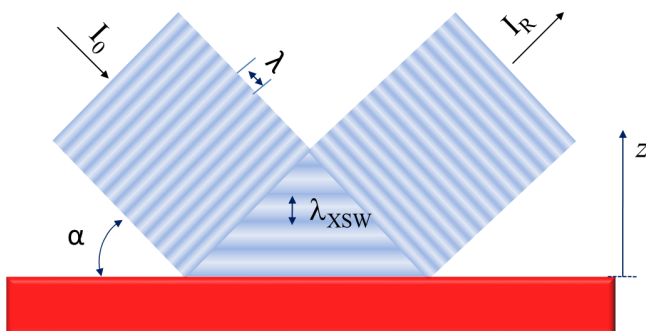
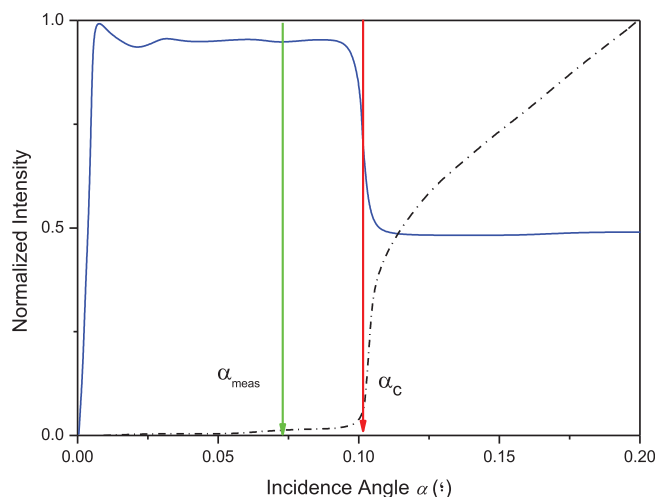


FIGURE 4 Cross-section of the X-ray Standing Waves field generated on the surface of a reflector below its critical angle



**FIGURE 5** Line blue displays the Fe fluorescence signal of a sample deposited as a film of 500 nm (Equation (5)) around the critical angle. The black line displays the background signal of a silicon reflector (Equation (6)) in the critical angle vicinity. The red arrow marks the critical angle  $\alpha_c$ . The green arrow marks the angle of measurements  $\alpha_{\text{meas}}$  assuring total-reflection X-Ray fluorescence condition. Excitation source of Mo K $\alpha$  (17.4 keV)

As Figure 5 shows, below the critical angle of the reflector  $\alpha_c$ , TXRF measurement region, the intensity of the fluorescence emission (blue) is approximately twice that of the higher angles, XRF measurement region. In the background intensity (black) below the critical angle  $\alpha_c$ , the spectral background contribution from the reflector decreases quickly because the intensity of the incident X-ray beam is reflected completely. The remaining intensity penetrates only a few nanometres in the reflector material. For angles above the critical angle  $\alpha_c$ , the contribution of the spectral background increases quickly and linearly. The spectral background decrease in a factor around 500. This minimisation is mainly due to measuring in the total-reflection region. If this reduction in the background is convoluted with factor two associated with the amplification of the elemental fluorescence signal below the critical angle, the signal-to-noise ratio obtained on the TXRF condition over conventional XRF is up to 3 orders of magnitude higher. Therefore, the resulting increase in sensitivity allows the TXRF to detect masses deposited on the reflector's surface of only a few picograms. In this way, if the measurement angle  $\alpha_{\text{meas}}$  is fixed approximately 70% of the critical angle  $\alpha_c$  (see Figure 5), the TXRF condition is assured. Consequently, the material deposition over the surface of a reflector allows the analysis of the element presents with the best signal to noise ratio and lower detection limits (DL) than the X-ray spectrometry can get today. From a physical perspective, this is the main differentiating factor of TXRF over conventional XRF spectrometries.

### 1.3 | Analytical background

TXRF is a “micro-analytical” technique because only small amounts of sample, around 0.1 to 10 micrograms, properly deposited on a reflector are analysed. The sample is deposited with a typical deposition thickness from 0.1 to 10  $\mu\text{m}$ , depending on the matrix type.<sup>[20]</sup> Under these conditions, the effects of absorption and secondary excitation are negligible, and the model of an infinitely thin film can be assumed. The great inherent advantage is that during the majority of the quantification process by TXRF matrix, effects can be neglected. From the analytical viewpoint, this characteristic is by far the biggest advantage that TXRF has over conventional XRF. As a result of minimising and even bypassing the matrix effect, the relative sensitivities in TXRF have a universal character, independently of the analysed matrix. Assess the relative sensitivities of a TXRF instrument is a relatively simple task. Figure 6 shows a TXRF spectrum of the deposition on a quartz reflector of 10  $\mu\text{L}$  of a multi-element pattern solution where the concentration of each element is 1 ppm (ng/ $\mu\text{L}$ ). Thus, the net mass of each element deposited was 10 nanograms. From certified standards, where the absolute mass of a deposited element can be known, it is easy to calculate each element's relative sensitivities. Evaluating the elemental range of TXRF, all elements with  $Z > 13$  can be analysed if the appropriate excitation source is used.

Elements with atomic numbers below  $Z = 13$  are difficult to evaluate with conventional TXRF instruments because their fluorescence emissions are of such low energy that they are absorbed quickly on their path from the sample to the detector. Only when samples with high Mg or Na concentration are analysed, these light elements can be evaluated. With the aims of increasing the range of lighter elements detected by TXRF, several instrumental improvements have been made, mainly by Peter Wobrauschek and Christina Strelí in the AtomInstitut of Vienna. This group has developed a special TXRF chamber, known as the “WOBISTRAX” chamber, capable of working under vacuum. In this way, combining this chamber with a high counting rate capacity detector (SDD), equipped with an ultra-thin window, and the use of a special source to optimise the excitation of low energy transitions, as Cr or a synchrotron line, is possible to analyse elements such as B, C, N, O, F, Na and Mg, with DL in the nanogram range by TXRF.<sup>[21]</sup>

Sample preparation in TXRF combines the versatility to analyse the same sample in different preparation ways. This fact gives TXRF a high analytical versatility to aboard complicated analytical problems. In a general approximation, liquid samples can be analysed directly to obtain a qualitative elemental profile. Then, the reference



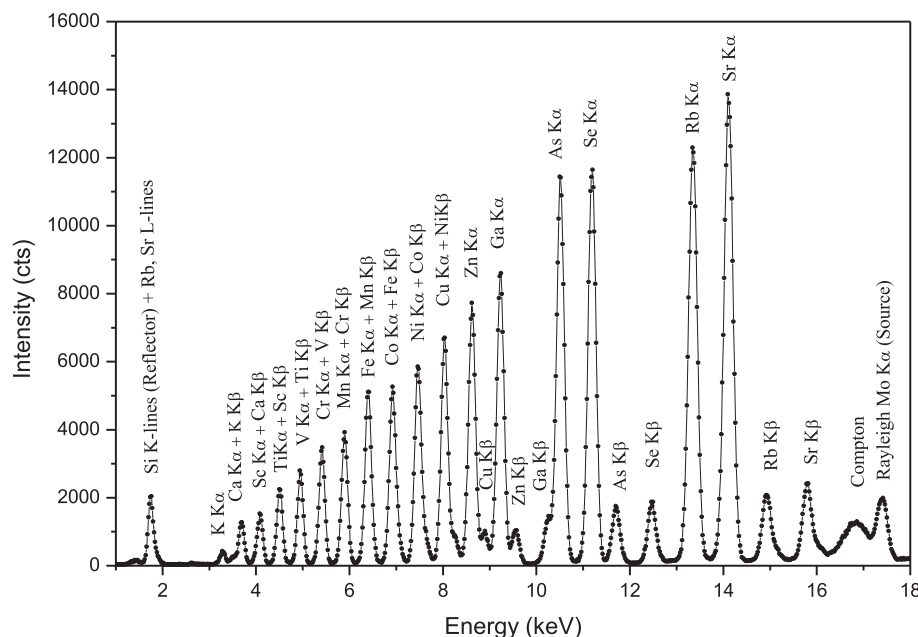


**FIGURE 6** Total-reflection X-Ray fluorescence spectrum of a multi-element pattern solution where the mass deposited for each element is 10 nanograms for an incident beam of Mo K $\alpha$  X-ray and acquisition time of 300 s. The spectrum shows the K-lines for each of the elements deposited, the Si signal from the quartz reflector, and Compton and Rayleigh's signal from the source

element is elected by its absence in the qualitative profile. The sample is standardised with a well-known concentration of the reference elements elected as internal standard and after it is deposited and analysed by TXRF. In the case of solids samples, they should be previously digested in an acid medium to obtain the solid's complete disaggregation as a general rule. Moreover, TXRF also allows the analysis of the same solid samples previous optimisation of the sample's solid suspension in an adequate liquid media, avoiding the complexity, cost, and dangerous of chemical acid digestion. In this way, TXRF allows a green analytical analysis. So, after acid digestion or suspension, the quantitation is the same as for a liquid sample.

From an analytical viewpoint, the TXRF have several significant advantages comparing with other more conventional techniques. Most importantly, once the relative instrumental sensitivities are known, their values remain unchanged for years and only need to be updated when the detection system or geometry is varied. Under these conditions, the TXRF shows all its potential in the atomic chemical analysis; this is, the simplicity of understanding, quantification and interpretation of the TXRF spectra. X-ray elemental analysis, within the angular region of total reflection, simplifies the main and non-trivial problem of conventional XRF quantitation, the non-linear matrix effect, in a simple and linear relation.<sup>[1]</sup> So, the master equation for quantification by TXRF comes given by the linear relationship

$$C_x = C_{\text{ref}} \frac{N_x}{N_{\text{ref}}} \frac{S_{\text{ref}}}{S_x}, \quad (7)$$

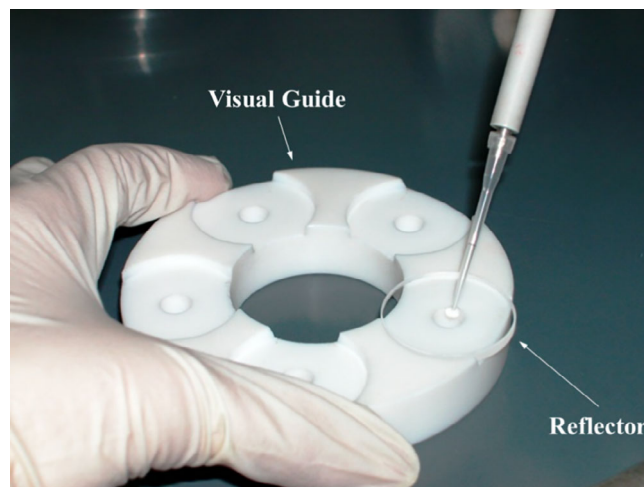


**FIGURE 7** Final deposition of an aliquot of the standardised sample on a quartz samples carrier and the basic tools for total-reflection X-Ray fluorescence analysis, a visual guide, a micropipette and a clean quartz reflector

where  $C_x$  and  $C_{\text{ref}}$  are the concentrations of element  $x$  and the internal standard ref,  $N_x$  and  $N_{\text{ref}}$  are their net intensities and  $S_x$  and  $S_{\text{ref}}$  are their sensitivities, respectively. As shown in Equation (7), the most suitable quantification method for the TXRF technique is the internal standard. This method is based on the addition of an aliquot of a known concentration of monoelemental pattern that is not present in the problem sample. So, the simple deposition of an aliquot of the standardised sample on a clean reflector (Figure 7) is enough to quantify the elements present in a problem sample solution.

The volume of sample deposited over reflector can be increased or decreased, within certain limitations imposed by the technique,<sup>[20]</sup> to get the best counting ratio in the process of acquiring the spectrum. Under these conditions, the measurable concentration range of TXRF can vary from a few ppbs to thousands of ppms, which implies an analytical concentration range of  $10^5$ , that is, five orders of magnitude from the higher to the lower concentration of the elements present in the problem sample analysed.

TXRF is a competing technique compared to AAS or ICP-OES because the DL for liquid samples are equivalent and vary from hundreds of ppt (ng/L) to dozens of ppb ( $\mu\text{g L}^{-1}$ ). Nevertheless, the ICP-MS technique is even more sensitive for liquid samples, with DL's about 1 ppt (ng/L) undoubtedly being more suitable for ultra-trace analysis than any other analytical technique. When analysing solid samples using TXRF, conventional treatment is the acid digestion of the sample, which is always required for the AAS and ICPS techniques. However, TXRF also allows a fast, simple and direct qualitative and mass proportion evaluation of the elements present in the analysed sample with only a few micrograms of sample and, more importantly, without chemical distortion due to acid digestion. Also, particle size modulation and suspension-assisted methods by ultrasonic techniques allow the quantitative evaluation of solids by TXRF.<sup>[22]</sup> This capability is one of the more valuable analytical properties that TXRF has and its inherent microanalytical characteristic.

One of TXRF analysis's major advantages is that it allows simultaneous qualitative inspection of the material's atomic fingerprint under investigation. This feature allows easy monitoring of processes by comparing their spectra in each of their phases. Moreover, the possibility of directly analysing a liquid or solid phase allows following the analysis process comprehensively. Consequently, this capability allows the simple evaluation of loss elements during the digestion process or the induction of impurities during the preparation process. The microanalytical character of the TXRF can be an advantage for certain types of studies and a disadvantage for adequately assessing a heterogeneous sample. For such samples, adequate homogenisation and statistical sampling are essential in sample preparation, in the same way that for any other analytical technique. One of the major disadvantages of TXRF compared to flame/plasma techniques is their extremely low sensitivities for the quantification of light elements  $Z < 13$  in conventional instruments.

On the other hand, quantification techniques such as AAS or ICPS require external calibration curves' performance. In contrast, the TXRF technique only requires an internal standard element addition of known

concentration, which is not present in the sample. This simplification of the quantification procedure means a considerable saving of time and costs during the analysis.

In terms of instrumentation costs, the "flame/plasma" techniques can be divided into three levels. Firstly, the level AAS, where the cost, including the graphite chamber, is about 60 K€. Secondly, the level Optic-Plasma (ICP-OES), where the costs vary around 90 K€. Finally, the level Mass-Plasma (ICP-MS), where the prices oscillate around 160 K€. In the case of the TXRF instruments for analytical applications, prices are also at different levels. The first is the cheaper TXRF WOBISTRAX vacuum chamber from the Atom Institute in Vienna, with prices around 50 K€. The second level is the robust TXRF spectrometer S2 PicoFox and the new S4 T-STAR, from Bruker-nano, next to the Horizon spectrometer from GNR, with prices from 70 to 100 K€. A third level is formed by the TXRF spectrometers with GIXRF capabilities, such as the NANO HUNTER-II spectrometer from Rigaku or the implemented S4 T-STAR from Bruker, with prices around 120 K€.

Today, TXRF instruments require a simple electrical plug. In contrast, flame or plasma technology mainly requires mainly high purity gases, among others, the price of which greatly increases the cost per sample compared to TXRF technology. This difference is the more outstanding since sample preparation, standardisation, purity, high purity reagents and materials are similar.

## 2 | GENERAL FIELDS OF APPLICATION

TXRF is a versatile technique, and the fields of applications where it can show its capabilities are wide. This section is intended to show some of the analytical fields in which TXRF has been applied successfully.

In the environmental field, the TXRF has been applied in many matrices to pollution control studies as real car three-way catalysts<sup>[23]</sup> or catalyst residues in active pharmaceutical ingredients.<sup>[24]</sup> In this field, the TXRF technique is suitable for analysing all types of water. So, it is possible to analyse drinking water,<sup>[25]</sup> river water,<sup>[26]</sup> rainwater<sup>[27]</sup> or even cloud water<sup>[28]</sup> to ppb's levels and only after the addition of an adequate internal standard (IS) of known concentration. Also, seawater or contaminated sludges can be analysed directly, after IS addition, to ppm's levels and even to ppb's levels if previously are removed the majority salts content and the matter in suspension.<sup>[29]</sup> Moreover, air pollution analysis due to suspended particles in aerosol form is a section where TXRF has begun to be applied with satisfactory results. Aerosol particles can be collected on environmental

survey stations on filter paper with different pore sizes, easily digested in acid.<sup>[30]</sup> However, more recent applications are based on cascade impactors that allow direct deposition of the aerosol's different size fractions on TXRF sample holder.<sup>[31]</sup> TXRF, among other techniques, was used to study the environmental problem of induction of uranium in crops grown on a mining site in Hungary.<sup>[32]</sup> Also, TXRF has been applied to studying different species of trees as bioindicators of pollution.<sup>[33]</sup> More recently, TXRF has shown to be a mature technique for environmental monitoring of an industrial site, performed using lichens as bioindicators.<sup>[34]</sup>

The industrial application is so far where TXRF has been more applied. The evaluation of superficial impurities in wafers used in microelectronics has been extensively studied by TXRF. So, methodologies for directly,<sup>[13]</sup> or using vapour phase decomposition (VPD-TXRF),<sup>[35]</sup> wafers contaminations have been developed. The industry of synthesis of new materials, such as lithium niobate tantalate in mixed-phase<sup>[12]</sup> or solid solutions of CuInSe:Ga<sup>[36]</sup> has also benefited from the versatility of TXRF for stoichiometric studies. TXRF has also studied microparticles and nanoparticle systems of high interest as novel catalytic materials,<sup>[37]</sup> luminescent materials<sup>[38]</sup> or voltaic pile.<sup>[15]</sup>

On the other hand, TXRF has also been involved in analysing products related to the consumer goods industry. There are applications developed in the wine industry to analyse metal contaminants in wines<sup>[39]</sup> or the oil industry for the analysis of crude oil fractionation processes.<sup>[40]</sup> Food analysis is a new line of application that last years is being explored for the TXRF technique.<sup>[41]</sup> Also, in the field of archaeological applications, the TXRF has been incorporated in very different facets. A very interesting review, written by Alex Von Bohlen, shows the versatility of the TXRF in solving complex archaeological problems.<sup>[42]</sup>

### 3 | BIOANALYTICAL APPLICATION

As a summary of the brief overview described so far, the TXRF has the following distinguishing features: micro-analytical capability, easy sample quantification by simply adding an internal standard, DL in the range of a few ppbs, reduced analysis time, minimal costs for analysis and instrument maintenance and finally the ability to analyse solids and liquids directly. For these reasons, the field of biomedical knowledge can find a strong ally in TXRF spectrometry. Nowadays, TXRF is not an extended technique frequently used in the biological and biomedical field. The number of applications is small, but it is

becoming more and more widespread. Kubala-Kukus et al.<sup>[43]</sup> and Szoboszlai et al.<sup>[44]</sup> conducted a compilation of biomedical and biological applications of TXRF, showing a complete overview of the research carried out in this field. Klockenkämper and Von Bohlen's reference work,<sup>[20]</sup> related to estimating the critical thickness and sensitivities of TXRF, gives the limits in mass and thickness deposited to work in TXRF condition for different matrices. In biosamples, these values can have a maximum thickness of 4 µm and a maximum dry mass of 40 µg. So, working under these values means a correct analytical quantification where intensity-concentration linearity can be ensured. In this line, Marcó and Hernández-Caraballo<sup>[45]</sup> applied TXRF to overcome the difficulties associated with biomedical samples analysis, particularly solid ones. So, a review of different procedures of sample preparation and calibration to approach the direct analysis were evaluated: slurry sampling, Compton peak standardisation, in situ microwave digestion, in situ chemical modification and direct analysis with internal standardisation for amniotic fluid, serum, urine and brain biomaterials.

#### 3.1 | Microtomic sections

One of the first applications of TXRF in the biomedical field was the ability of direct analysis of microtomic sections of biomedical and vegetable tissues, developed by Klockenkämper et al.<sup>[46]</sup> Samples were prepared using a freezing microtome with a thick around 10 µm and a wet mass of around 200 micrograms directly deposited on a quartz reflector and spiked with 10 nanograms of Ga. The method was applied to vegetable and animal foodstuff (nuts, mushrooms, shrimps) and various tissues (liver, human lung). Quantitative results, in the range from 200 ppb to 700 ppm, were achieved for Zn, Mn, Fe, Cu, Br, As, Sr, Rb, Se, and Ni. More recently, Magalhães et al.<sup>[47]</sup> applied this methodology to investigate the elemental distribution of P, S, Cl, K, Ca, Cr, Mn, Fe, Ni, Cu, Zn, Se, Br, Rb, Sr and Pb, in normal and cancerous tissues. In particular, colon, breast and stomach.

#### 3.2 | Human fluids

##### 3.2.1 | Blood-serum

One of the first approximations to the analysis of blood using TXRF was the analysis of Pb in blood was investigated by Ayala et al.<sup>[48]</sup> for two kinds of donors; one occupationally exposed to lead contamination in a car battery factory and other unexposed. The analysis was



performed by the addition of 5 ppm of Sr as internal standard, the deposition of 2  $\mu$ L on a quartz reflector and ashed in a low-temperature oxygen plasma. The elements detected in blood were K, Ca, Ti, Cr, Fe, Ni, Cu, Zn, Pb, Rb and Sr. The DL achieved for Pb was of 30 ppb. Occupationally exposed donors clearly show higher lead concentrations, between 230 and 680 ppb, than unexposed individuals with concentrations lower than 100 ppb. Savage et al.<sup>[49]</sup> also investigated the effect of chemical modifiers in analysing blood plasma by TXRF. They analyse the elements As, Br, Cd, Ca, Cl, Co, Cu, I, Fe, Pb, Mn, Mo, Ni, Se, Sn and Zn in a concentration range from 1 ppb to 270 ppm.

One of the most common analytical tasks about inorganic traces in clinical service laboratories is the determination of the nutrition-relevant elements Fe, Cu, Zn and Se. Stonach and Mages<sup>[50]</sup> showed that TXRF could be applied in human blood and serum only by dilution and internal standardisation of the samples for the routine analysis of the nutrition-relevant elements.

An interesting study related to the investigation of element levels in human serum was recently developed by Majewska et al.<sup>[51]</sup>. The study's purpose was to determine the concentration levels of several elements (P, S, Cl, K, Ca, Cr, Fe, Cu, Zn, Se, Br, Rb, Pb) in human serum and to define their reference values. More recently, Pierzak et al.<sup>[52]</sup> used TXRF to determine chromium, selenium and bromine concentrations in blood serum samples of 50 patients with parenteral nutrition treatment. For comparison purposes, serum samples of 50 patients without nutritional disorders were analysed and treated as the control group. The main conclusion was that the TXRF technique could be successfully used to monitor the concentration of the relevant trace elements in human serum in parenteral nutrition treatment.

### 3.2.2 | Amniotic fluid

Carvalho et al.<sup>[53]</sup> applied TXRF to the study of human amniotic fluid and placenta to correlate the metal contents with the newborn infant weight and maternal age. Very low Ni and Sr levels were found in the amniotic fluid samples, and their contents were independent of the age of the mother and the child's weight. Zn was not significantly different in the samples analysed; however, it was weakly related to birth weights. Ca and Fe were significantly correlated with the mother's age and newborn weight. Recently, Marguá et al.<sup>[54]</sup> applied TXRF as a cost-effective multielemental analytical technique for the human placenta and amniotic fluid analysis. An easy and rapid sample preparation consisting of the sample suspension was compared with acid digestion and

ICP-AES procedure. Most elements' DL were in the low mg/kg level for both sample treatment methodologies. Accurate and precise TXRF results were obtained using internal standardisation as a quantification approach and applying a correction factor to compensate for absorption effects.

### 3.2.3 | Cerebrospinal fluid

Cerebrospinal fluid was studied by TXRF by Ostachowicz et al.<sup>[55]</sup>, particularly in the study of the neurodegenerative disease amyotrophic lateral sclerosis (ALS). Samples of the cerebrospinal fluid from two groups of patients, ALS and control, were analysed. The elements Cl, K, Ca, Cr, Mn, Fe, Ni, Cu, Zn, Rb and Br were evaluated. The study showed differences in the concentrations of Zn and Cl between the ALS and the control group.

### 3.2.4 | Oral fluid

Oral fluids also were evaluated by TXRF, and one of the first studies was made by Abraham et al.<sup>[56]</sup>. This work presents the study of the elemental composition of oral fluids such as saliva and gingival crevice fluid, and their relation with smoking. Two sets of patients, smokers and non-smokers were selected according to certain criteria to analyse saliva and gingival crevice fluid. The most significant differences in concentration between smokers and non-smokers were found in saliva samples for S, K and Ca. More recently, the same group of Abraham et al.<sup>[57]</sup> applied TXRF spectrometry in an indirect study of corrosion of dental implants by analysing changes in metals' elemental concentration in oral fluids. Degradation of the implant surface releases material to the medium, which, depending on the concentrations, can represent a toxic risk, organic malfunction, pain, rejection, etc. The concentrations of representative metals such as Ti, Al, and V in saliva and gingival fluids were analysed, employing total reflection of X-rays fluorescence analysis using synchrotron radiation to evaluate the degradation process.

### 3.2.5 | Urine

One of the first applications of TXRF to the study of urine fluid was developed by Zarkadas et al.<sup>[58]</sup> In this reference work, trace uranium content was determined by TXRF. The method utilises open vessel digestion with nitric acid and uranium preconcentration by using sodium dibenzoyldithiocarbamate (NaDBDTC) as the complexing

agent. Employing the developed procedure DL around 1 ppb were obtained with recoveries around 100% and uncertainties lower than 10%. Telgmann et al.<sup>[59]</sup> developed a simple and rapid method to determine gadolinium (Gd) concentrations in urine and blood plasma samples using TXRF. The achieved limits of detection were  $100 \mu\text{g L}^{-1}$  in urine and  $80 \mu\text{g L}^{-1}$  in blood plasma, and the limits of quantification of  $330 \mu\text{g L}^{-1}$  in urine and  $270 \mu\text{g L}^{-1}$  in blood plasma. The TXRF methodology allows analysing urine samples taken from magnetic resonance imaging (MRI) patients during a period of up to 20 hr after the administration of Gd-based MRI contrast agents. So, urine analysis combined with the blood Gd evaluation makes it possible to monitor Gd's excretion kinetics from the patient's body. More recently, Majewska et al.<sup>[60]</sup> applied TXRF to define the reference values of elemental concentration in human urine. For this purpose, a set of certified human urine and real samples was employed. All of the parameters affecting sample preparation and measurement conditions were carefully evaluated, and finally, the procedure for optimal urine preparation and optimal measurement conditions was defined. As results, the reference values of concentration of several elements (K, Ca, Cr, Mn, Fe, Ni, Cu, Zn, Br, Rb and Sr) were defined based on the analysis of 100 urine samples. The observed correlations were as follows. First, higher values than the median for Ca, Cr, Zn, Rb and Sr in men urine than in women urine; second, lower values than the median concentration of Mn in men urine than in women urine and third, lower values than the median for Zn, Rb, and Sr for both older men and women.

### 3.2.6 | Seminal fluid

Camejo et al.<sup>[61]</sup> applied for the first time TXRF in the research of human sperm. In particular, to determine the concentrations of Se, Cu, and Zn in the semen of patients with varicocele and the relationship with seminal parameters. As the main conclusion, a decrease in selenium concentration was associated with the detriment of seminal parameters: spermatozoa concentrations, motility and morphology. More recently, Margui et al.<sup>[62]</sup> have presented a simple and reliable method for determining several elements in seminal plasma samples by using TXRF. Applying the best analytical conditions, DL for trace elements were in the range of 0.04–0.3 mg/kg. Trueness and precision of the results, evaluated by spiked seminal sample analysis, were in most cases acceptable with recoveries values in the range of 87%–109% and relative SDs 3%–12% ( $n = 5$ ). Among the studied trace elements with a role in the antioxidant

defence system, only Zn could be quantified, and some differences in Zn concentrations among studied groups were observed.

## 3.3 | Metalloproteins

Wittershagen et al.<sup>[63]</sup> developed a procedure for the determination of metal cofactors in respiratory chain complexes by TXRF. The two-terminal oxidase, cytochrome c oxidase and quinol oxidase, isolated from the soil bacterium *Paracoccus denitrificans*, were transferred from their usual saline buffer into a solution of 100 mmol/L tris(hydroxymethyl)aminomethane acetate (TRIS) with 0.02% of Triton X. By this procedure an improved signal/noise ratio was obtained. Without any decomposition, elements Fe, Ni, Cu, Zn, Mn and Mo could be determined with high accuracy. Moreover, sulfur could be determined in protein samples. Wellenreuther et al.<sup>[64]</sup> investigated the best conditions for the analysis by TXRF of the followings metalloproteins; hELAC1, insulin, concanavalin A, thermolysin and glucose isomerase. The study's main conclusion was that elaborate sample decomposition is not generally necessary; instead, direct analysis of proteins samples is feasible. More recently, Strohmidel et al.<sup>[65]</sup> investigated the binding of ethylmercury ( $\text{EtHg}^+$ ) released from the preservative thiomersal by hydrolysis to proteins in influenza vaccines via ultrafiltration and subsequent TXRF analysis as well as size exclusion chromatography (SEC) hyphenated to inductively coupled plasma-mass spectrometry (ICP-MS).

## 3.4 | Cytosol-pellet

An interesting application related to the first approximation to intracellular speciation of vegetal cells was developed by Günther et al.<sup>[66]</sup>. In this case, TXRF was used for the simultaneous determination of Ca, Cu, Fe, K, Mn, Rb, Sr and Zn in 12 different vegetable foodstuffs and their cell fractions after mechanical cell breakdown. The homogenates were separated into the cytosol (liquid fraction) and pellets (solid fraction) by centrifugation. Before their analysis by TXRF, samples were digested with nitric acid and spiked with Ga as an internal standard. In the study, each of the fractions' elemental distributions were determined, obtaining that, on average Sr, Ca, and Fe were mainly bound to pellet components. In this line, Gonzalez et al.<sup>[67]</sup> used for the first time the TXRF technique for the determination of Cu, Fe, Zn, Ca and S in different types of tumoral mammalian cultured cells; human clonal cell lines HepG2, Caco-2 and HeLa, clonal

cell lines from mice NIH 3 T3 and N2A and finally, a clonal cell line from rats B12. The work's goals were to evaluate their elemental distribution, intracellular concentrations and the changes induced in their proportions when cells were chronically exposed to copper. Results indicate that TXRF allows detecting total trace metal contents using a minimum amount of cells  $(1-2) \times 10^6$  while  $(4-6) \times 10^6$  cells were sufficient to determine their cytosol/pellet distribution.

### 3.5 | Cancer research

#### 3.5.1 | Antitumoral compounds action

TXRF was applied for monitoring the molecular introduction kinetic of the Pt-Berenil and *cis*-DDP compounds that take place when crossing the biological barrier of the HeLa cells applying TXRF by Fernández-Ruiz et al.<sup>[68]</sup>. The medicines which interact with the DNA on the nucleus were also quantified. This work opened the intracellular metal studies in conjunction with a good subcellular constituent separation technique by TXRF. A sample volume of only 100  $\mu$ L with Pt concentrations from 3 to 30 ng/mL was determined with a relative *SD* between 2% and 8%. Recently, a similar study was developed by Majer et al.<sup>[69]</sup> for dinuclear Rh(II) complexes of phenylalanine derivatives as potential anticancer agents of colon carcinoma. Depending on the complex ligand type and its coordination number, the intracellular rhodium (Rh) content determined by TXRF spectrometry in the human colon HT-29 cells varied between 25 and 2,500 ng/ $10^6$  cells.

#### 3.5.2 | Tumoral-cancerous tissues

The study of healthy and cancerous tissues has been extensively investigated by using TXRF. One of the first studies developed in this line was reported by Czarnowski et al.<sup>[70]</sup> in 1997. This pioneering study intended to establish a new methodology for cancer diagnosis. For this purpose, different trace elements distributions in carcinomas of the digestive tract and normal tissues of the human stomach, colon and rectum in correlation with the type of cancer were determined by TXRF analysis. A significant diminution of Cr, Fe and Ni in carcinoma of the stomach, of Cr and Co in carcinoma of the colon and a significant accumulation of K in cancerous tissue of the colon and of Fe and K in neoplastic tissue of the rectum were discovered for a very limited population of patients. Li et al.<sup>[71]</sup> studied the changes of trace elements in lung cancer cells and cervix cancer before and

after apoptosis by using the implemented line of TXRF in the Beijing synchrotron. Magalhães et al.<sup>[72]</sup> investigated the elemental distribution of P, S, Cl, K, Ca, Cr, Mn, Fe, Ni, Cu, Zn, Se, Br, Rb, Sr, I and Pb in normal and cancerous tissues of the same individual along several adjacent thin sections of each tissue. Carcinoma tissues of colon, breast and uterus on seven citizens from the German population, were analysed directly by TXRF. By the same processes, 10 carcinoma samples of 10 Portuguese citizens from rectum, sigmoid, thyroid, kidney, larynx and lung were evaluated to find out a similar correlation pattern in the studied elements in carcinoma tissues. A similar pattern for all the analysed tissues was obtained: increased or constants levels of P, S, K, Ca, Fe and Cu and decreased levels of Zn and Br were found in carcinoma tissues, when compared with the corresponding healthy ones. Carvalho et al.<sup>[73]</sup> conducted an interesting summary of studies on elemental profiles between healthy and cancerous human for breast, lung, serum, intestinal, prostate and uterus tissues carried out by TXRF. Szoboszlai et al.<sup>[74]</sup> developed a procedure for the direct elemental analysis of cancer cell lines by TXRF using the deposition of tumoral or health cells directly on the TXRF reflector. In these conditions, the method was applied to human colon adenocarcinomas and the levels of Cu, Zn and Fe were evaluated. Leitão et al.<sup>[75]</sup> applied TXRF to evaluating the elemental profile P, S, K, Ca, Fe, Cu, Zn and Rb in health and tumoral human prostate tissues to find diagnostic strategies.

### 3.6 | Vegetal cell system

Mages et al.<sup>[76]</sup> analysed biofilm as bioindicators of polluted water by using TXRF. They found differences in concentration of several orders of magnitude between biofilms grown in polluted water and grown in unpolluted waters. The elements evaluated were K, Ca, Cr, Mn, Fe, Ni, Cu, Zn, As and Sr with masses of the sample between 10 and 500  $\mu$ g and DL of only some ppb. Woelfl et al.<sup>[77]</sup> applied TXRF to the study of trace metals in planktonic microcrustacean. The mass of sample evaluated was lower to 50  $\mu$ g, and the elements Mn, Fe, Ni, Cu, Zn and As were studied at ppm levels. Pepponi et al.<sup>[78]</sup> applied TXRF to the study of pollen as a bioindicator for atmospheric pollution for the *Corylus avellana* L. (hazel) pollen collected in five sites of the province of Trento, Italy with different anthropic impact. The elements Al, P, S, K, Ca, Ti, V, Cr, Mn, Fe, Ni, Cu, Zn, Br, Rb, Sr, Ba and Pb were evaluated, and DL in the ppb range were obtained.

Mosses were early evaluated as promise candidates for environmental pollution evaluation. One of the first

studies by TXRF was developed by Market et al.<sup>[79]</sup> The moss samples of three different species were analysed for trace elements using TXRF spectrometry. Approximately 20 elements were determined, with DL typical of the order of 0.2–0.5 µg/g. The moss samples' results showed strong variations in the pollution with hazardous metals, depending on the type of sampling site. Some samples demonstrated the feasibility of TXRF analysis for the routine monitoring of plant samples. More recently, simplified methodologies, by using previous suspension and internal standardisation of the analyses mosses or the more conventional previous acid digestion, has been applied with success in the environmental pollution evaluation of the city of Mexico (Toluca Valley) by Zarazua-Ortega et al.<sup>[80]</sup> or Paris by Natali et al.<sup>[81]</sup>. Espinoza-Quñones et al.<sup>[82]</sup> studied the bioaccumulation kinetics of lead by living aquatic macrophyte *Salvinia auriculata* by TXRF. According to the experimental data, both adsorption and bioaccumulation mechanism was present, and competition between P macronutrient and Pb for plant growth was observed when the great concentration of lead in roots was present. More recently, Höhner et al.<sup>[83]</sup> develop a rapid protocol by TXRF that allows the simultaneous quantification of several elements such K, Ca, S, Mn and Sr in *Arabidopsis thaliana* leaf specimens. The ion homeostasis of macro- and micronutrients in plant cells and tissues is a fundamental requirement for vital biochemical pathways, including photosynthesis. TXRF represents a powerful method to gain detailed quantitative insights into (I) the effect of environmental stress on plant ion homeostasis, (II) ion gradients between plant tissues, and (III) ion levels in plant mutants with compromised growth or heterogeneous phenotypes.

### 3.7 | Microbiological systems

TXRF spectrometry was applied to evaluate the kinetic behaviour of the Cr(VI) bioaccumulation process of the bacterium ANCR (*Acinetobacter beijerinckii* type) by Fernández-Ruiz et al.<sup>[84]</sup>. The results demonstrate that this new strain of *Acinetobacter* bacterium can reduce the chromium present in the culture medium. Consequently, it can be used as a promising microorganism for Cr(VI) bioremediation from polluted wastewaters. Additionally, this work shows clearly the versatility, potential and sensitivity of TXRF spectrometry for the analytical evaluation of metals in this kind of microbiological systems.

Fiedor et al.<sup>[85]</sup> applied TXRF spectrometry to perform a comprehensive analysis of the trace elements content of purple non-sulfur phototrophic bacteria, their chromatophores and selected photosynthetic structures

in response to alterations in oxygen growth conditions. There is a lack of consistent information on microelements' content, distribution, and correlations between them. The analysis carried out on the *Rhodobacter sphaeroides* species aims to rectify this. Qualitative examination revealed the presence of microelements generally not considered as basic in the bacterial ionome. Quantitative inspection pointed to Fe as the major trace element in this phototrophic species irrespective of growth conditions (sample type). The ionic approach to elemental accumulation followed by statistical analysis revealed intriguing relationships between the elements within cells and phototrophic membranes. The vast potential and usefulness of the TXRF technique in a wide range of biological and environmental applications are underlined.

### 3.8 | Medical nanoparticles

Suspension of magnetic nanoparticles in aqueous media attracts much interest because of their potential for many applications in the biomedicine field,<sup>[86]</sup> including biomolecules separation, MRI or drug delivery. Fernandez-Ruiz et al.<sup>[87]</sup> developed a procedure for the analysis of Fe and traces metals in functionalised magnetite nanoparticles, used as an image contrast agent for NMR, without sample digestion and in a direct solid way by TXRF. Antosz et al.<sup>[88]</sup> published an introduction of the TXRF technique applied to the pharmaceutical industry community. This work shows that the results obtained by TXRF were comparable with those obtained by ICP-MS for the same samples for Pd and Cu measurement, and statistical analysis indicated that the results obtained by the two technologies were equivalent at the 95% confidence level.

Gold nanoparticles (AuNPs) have several biomedical applications, but the impact of these nanoparticles in the human organism is not yet well-understanding. One of the first approximations to the gold nanoparticles evaluation by TXRF was developed by Fernández-Ruiz et al.<sup>[89]</sup> They evaluated the bioaccumulation kinetics of gold nanorods (AuNRs) in various organs upon intravenous administration in mice. The AuNRs bioaccumulation kinetics was analysed in several vital mammalian organs such as the liver, spleen, brain, and lung at different times. Also, urine samples were analysed to study the kinetics of eliminating the AuNRs by this excretion route. The main achievement was differentiating two kinds of behaviours. AuNRs were quickly bioaccumulated by highly vascular filtration organs, such as liver and spleen, while AuNRs do not show a bioaccumulation rate in brain and lung for the period investigated. TXRF proved



to be a powerful, versatile, and precise analytical technique for the evaluation of AuNPs content in biological systems and, in a more general way, for any kind of metallic nanoparticles. More recently, Mankovskii and Pejović-Milić<sup>[90]</sup>, have applied TXRF to the validation of a TXRF-based quantification method for trace-level gold nanoparticles in an organic matrix. Suitable internal standards, fitting approaches and sample preparation methods that yield acceptable recovery rates were investigated. The developed method was validated with reference material nanoparticles. Recovery rates of  $(102.7 \pm 3.7)\%$  and  $(100.9 \pm 5.1)\%$  were achieved for nanoparticles in an ionic solution and organic matrix, respectively. These results suggest that TXRF is a good technique to quantify gold nanoparticle uptake in cancer cells accurately.

### 3.9 | Ions in molecular layers

Zheludeva et al.<sup>[91,92]</sup> took advantage for the first time of the angle dependence of the XSW field to study molecular monolayers. This use enables to localise ions in the monolayer versus the film-liquid interface by analysing the angular curves of their characteristic fluorescence radiation around the critical angle. This method's possibilities were considered on phthalocyanine, cycloliner polyorganoxilanes and phospholipid of Langmuir layers on the surface of a liquid and a protein-lipid film based on Ca-ATPase on a solid substrate. This work opened a new field of application of angle-dependent TXRF to the study of diffusion of metals in systems interfaces. More recently, Brücher et al.<sup>[93]</sup> applied the angle-dependent TXRF to evaluate functionalised solid-liquid interfaces by XSW combined with streaming current measurements to study surface charges, interfacial potential, and ion distributions. Thin films of an aqueous solution containing  $\text{Br}^-$  anions and  $\text{Fe}^{3+}$  cations at a concentration of 10 mg/L were prepared on functionalised silicon wafers. The ion distribution was measured with nanometer resolution, distinguishing between absorbed and mobile ions at the surface and in the diffusive layer, respectively.

One of the last applications developed in the biomedical field by TXRF has been its use for the predictive study of the survival rate in COVID-19 from the biomarkers Zn and Se in human serum.<sup>[94]</sup> The combination of serum Zn and Seleloprotein P concentrations versus patient age as a new composite parameter of trace element metabolism provides valuable information on the prognosis of COVID-19 patients. Concentrations within the reference ranges indicate high chances of survival, while substantial deficiencies cause concern and consideration of supplemental provision. It is currently unknown whether

correcting a strong trace element deficit in sick patients supports convalescence in COVID-19, so further studies are necessary.

## 4 | CONCLUSIONS

The great diversity of fields in which TXRF has so far demonstrated its analytical capabilities shows the wide range of applications in which it can be applied successfully, with minimal cost and maximum analytical potential. Nowadays, TXRF is an instrumental technique that is being active each time more, from its development, implementation, and application in all fields of scientific knowledge. Their simple and basic principles make TXRF a very versatile technique, capable of approaching the analysis of complex matrices with relative ease. The fields of application where TXRF can show its analytical capacity are still many. Its application to the best understanding of biomedical, biological or biochemical problems is a promise and open field where TXRF can still play an important role in understanding cytotoxicity, drug release, chemical equilibrium processes in cellular systems or metallomics, among others.

## ACKNOWLEDGEMENTS

The authors are thankful to the Autonomous University of Madrid (UAM) for instrumental and personal support. This article is into the frame of the COST Action CA18130 ENFORCE TXRF, supported by COST (European Cooperation in Science and Technology).

## DATA AVAILABILITY STATEMENT

Data sharing does not apply to this article, as no new data were created or analysed in this study.

## ORCID

Ramón Fernández-Ruiz  <https://orcid.org/0000-0003-4769-3484>

## REFERENCES

- [1] R. Klockenkämper, A. Von Bohlen, *Total-Reflection X-ray Fluorescence Analysis and Related Methods*, 2nd ed., John Wiley & Sons, Hoboken, NJ **2015**.
- [2] ENFORCE-TXRF COST Action CA18130 WEB page: <http://www.enforcetxrf.eu>.
- [3] A. H. Compton, *Philos. Mag.* **1923**, 45, 1121.
- [4] Y. Yoneda, T. Horiuchi, *Rev. Sci. Instrum.* **1972**, 42, 1069.
- [5] H. Aiginger, P. Wobrauschek, *Nucl. Instrum. Methods* **1974**, 114, 157.
- [6] H. Aiginger, P. Wobrauschek, *Anal. Chem.* **1975**, 47, 852.
- [7] H. Schwenke, J. Knoth, *Nucl. Instrum. Methods* **1982**, 193, 239.
- [8] K. Tsuji, J. Injuk, R. Van Grieken, *X-ray spectrometry: Recent technological advances*, Wiley, Chichester, UK **2004**.

- [9] B. Shaw, D. J. Semin, M. E. Rider, M. R. Beebe, *J. Pharm. Biomed. Anal.* **2012**, 63, 151.
- [10] R. Fernández-Ruiz, M. Furió, F. Cabello Galisteo, C. Larese, M. López Granados, R. Mariscal, J. L. G. Fierro, *Anal. Chem.* **2002**, 74, 5463.
- [11] R. Fernández-Ruiz, M. Garcia-Heras, *Spectrochim. Acta Pt B.* **2008**, 63, 975.
- [12] R. Fernández-Ruiz, V. Bermudez, *Spectrochim. Acta Pt B.* **2005**, 60, 231.
- [13] C. Neumann, P. Eichinger, *Spectrochim. Acta Pt B.* **1991**, 46, 1369.
- [14] R. Klockenkämper, A. Von Bohlen, L. Moens, *X-Ray Spectrom.* **2000**, 29, 119.
- [15] R. Fernández-Ruiz, P. Ocon, M. Montiel, *J. Anal. At. Spectrom.* **2009**, 24, 785.
- [16] R. Dalipi, E. Marguá, L. Borgese, L. E. Depero, *Food Chem.* **2017**, 218, 348.
- [17] A. Von Bohlen, *Spectrochim. Acta Pt B.* **2009**, 64, 821.
- [18] R. Van Grieken, A. Markowicz, *Handbook of X-Ray Spectrometry*, Marcel Dekker, New York **2002**.
- [19] M. J. Bedzyk, G. M. Bommarito, J. S. Schildkraut, *Phys. Rev. Lett.* **1989**, 62, 1376.
- [20] R. Klockenkämper, A. Von Bohlen, *Spectrochim. Acta Part B.* **1989**, 44, 461.
- [21] C. Strelí, P. Wobrauschek, G. Pepponi, N. Zoeger, *Spectrochim. Acta Pt B.* **2004**, 59, 1199.
- [22] R. Fernández-Ruiz, E. J. Friedrich, M. J. Redrejo, *Spectrochim. Acta Pt B.* **2018**, 140, 76.
- [23] R. Fernández-Ruiz, C. Larese, F. Cabello Galisteo, M. López Granados, R. Mariscal, J. L. G. Fierro, *Analyst* **2006**, 131, 590.
- [24] E. Marguá, I. Q. Mitjans, M. Hidalgo, *Spectrochim. Acta Pt B.* **2013**, 86, 50.
- [25] A. Prange, J. Knoth, R. P. Stöbel, H. Böldeker, K. Kramer, *Anal. Chim. Acta* **1987**, 195, 275.
- [26] A. Prange, H. Böldeker, K. Kramer, *Spectrochim. Acta Pt B.* **1993**, 48, 207.
- [27] R. P. Stöbel, A. Prange, *Anal. Chem.* **1985**, 57, 2880.
- [28] K. W. Fomba, N. Deabji, S. E. I. Barcha, E. M. E. IbrahimOuchen, R. C. El Moursli, S. E. H. MimounHarnafi, A. Mellouki, H. Herrmann, *Atmos. Meas. Tech.* **2020**, 13, 4773.
- [29] A. Prange, A. Knöchel, W. Michaelis, *Anal. Chim. Acta* **1985**, 172, 79.
- [30] S. Motellier, K. Lhaute, A. Guiot, L. Golanski, C. Geoffroy, F. Tardif, *J. Phys. Conf. Ser.* **2011**, 304, 012009.
- [31] T. Stahlschmidt, M. Schulz, W. Dannecker, *Spectrochim. Acta Pt B.* **1997**, 52, 995.
- [32] A. Alsecz, J. Osán, S. Kurunczi, B. Alföldy, A. Varhegyi, S. Török, *Spectrochim. Acta Pt B.* **2007**, 62, 769.
- [33] A. E. S. de Vives, S. Moreira, S. Brienza, J. G. Medeiros, M. Tomazello Filho, O. Zucchi, V. do Nascimento Filho, R. Barroso, *Nucl. Instrum. Methods Phys. Res. A* **2007**, 579, 494.
- [34] L. Borgese, A. Zacco, E. Bontempi, P. Colombi, R. Bertuzzi, E. Ferretti, S. Tenini, L. E. Depero, *Meas. Sci. Technol.* **2009**, 20, 084027.
- [35] S. Ayako, M. Kunihiro, M. Tsuyoshi, I. Shoko, *Jap. J. Appl. Phys.* **2006**, 45, 9037.
- [36] R. Fernández-Ruiz, J. P. Cabañero, E. Hernandez, M. León, *Analyst* **2001**, 126, 1797.
- [37] R. Fernández-Ruiz, R. Andrés, E. de Jesús, P. Terreros, *Spectrochim. Acta Pt B.* **2010**, 65, 450.
- [38] R. Fernández-Ruiz, J. C. Rodríguez-Ubis, A. Salvador, E. Brunet, O. Juanes, *J. Anal. At. Spectrom.* **2010**, 25, 1882.
- [39] M. L. Carvalho, M. A. Barreiros, M. M. Costa, M. T. Ramos, M. I. Marques, *X-Ray Spectrom.* **1996**, 25, 29.
- [40] N. Ojeda, E. D. Greaves, J. Alvarado, L. Sajo-Bohus, *Spectrochim. Acta Pt B.* **1993**, 48, 247.
- [41] L. Borgese, F. Bilo, R. Dalipi, E. Bontempi, L. E. Depero, *Spectrochim. Acta Pt B.* **2015**, 113, 1.
- [42] A. Von Bohlen, *e-PS* **2004**, 1, 23.
- [43] A. Kubala-Kukuś, J. Braziewicz, M. Pajek, *Spectrochim. Acta Pt B.* **2004**, 59, 1283.
- [44] N. Szoboszlai, Z. Polgári, V. G. Mihucz, G. Záray, *Anal. Chim. Acta* **2009**, 633, 1.
- [45] P. Lué Merlú Marcó, E. A. Hernández-Caraballo, *Spectrochim. Acta Pt B.* **2004**, 59, 1077.
- [46] R. Klockenkämper, A. Von Bohlen, B. Wiecken, *Spectrochim. Acta Pt B.* **1989**, 44, 511.
- [47] T. Magalhães, M. L. Carvalho, A. Von Bohlen, M. Becker, *Spectrochim. Acta Pt B.* **2010**, 65, 493.
- [48] R. E. Ayala, E. M. Alvarez, P. Wobrauschek, *Spectrochim. Acta Part B.* **1991**, 46, 1429.
- [49] I. Savage, S. J. Haswell, *J. Anal. At. Spectrom.* **1998**, 13, 1119.
- [50] H. Stosnach, M. Mages, *Spectrochim. Acta Pt B.* **2009**, 64, 345.
- [51] U. Majewska, P. Łyżwa, K. Łyżwa, D. Banaś, A. Kubala-Kukuś, J. Wudarczyk-Moćko, I. Stabrawa, J. Braziewicz, M. Pajek, G. Antczak, B. Borkowska, S. Góźdź, *Spectrochim. Acta Pt B.* **2016**, 122, 56.
- [52] M. Pierzak, A. Kubala-Kukuś, D. Banaś, I. Stabrawa, J. Wudarczyk-Moćko, S. Gluszek, *PLoS One* **2020**, 15, e0243492.
- [53] M. L. Carvalho, P. J. Custodio, U. Reus, A. Prange, *Spectrochim. Acta Pt B.* **2001**, 56, 2175.
- [54] E. Marguá, P. Ricketts, H. Fletcher, A. G. Karydas, A. Migliori, J. J. Leani, M. Hidalgo, I. Queralt, M. Voutchkov, *Spectrochim. Acta Pt B.* **2017**, 130, 53.
- [55] B. Ostachowicz, M. Boruchowska, M. Lankosz, B. Tomik, A. Szczudlik, D. Adamek, *X-Ray Spectrom.* **2004**, 33, 46.
- [56] J. A. Abraham, H. J. Sanchez, M. C. Valentinuzzi, M. S. Grenón, *X-Ray Spectrom.* **2010**, 39, 372.
- [57] J. A. Abraham, H. J. Sánchez, M. S. Grenón, C. A. Pérez, *X-Ray Spectrom.* **2014**, 43, 193.
- [58] C. Zarkadas, A. G. Karydas, T. Paradellis, *Spectrochim. Acta Pt B.* **2001**, 56, 2505.
- [59] L. Telgmann, M. Holtkamp, J. Künnemeyer, C. Gelhard, M. Hartmann, A. Klose, M. Sperling, U. Karst, *Metallomics* **2011**, 3, 1035.
- [60] U. Majewska, P. Łyżwa, A. Kubala-Kukuś, D. Banaś, J. Wudarczyk-Moćko, I. Stabrawa, S. Góźdź, *Spectrochim. Acta Pt B.* **2018**, 147, 121.
- [61] M. I. Camejo, L. Abdala, G. Vivas-Acevedo, R. Lozano-Hernández, M. Angeli-Greaves, E. D. Greaves, *Biol. Trace Elem. Res.* **2011**, 143(3), 1247.
- [62] E. Marguá, J. Dumić, I. Queralt, L. Baković, J. Jablan, *Anal. Methods* **2020**, 12, 4899.
- [63] A. Wittershagen, P. Rostam-Khani, V. Zickermann, I. Zickermann, S. Gemeinhardt, B. Ludwig, B. O. Kolbesen, *Fresenius J. Anal. Chem.* **1998**, 361, 326.

- [64] G. Wellenreuther, U. E. A. Fittschen, M. E. S. Achard, A. Faust, X. Kreplin, W. Meyer-Klaucke, *Spectrochim. Acta Pt B.* **2008**, *63*, 1461.
- [65] P. Strohmidel, M. Sperling, U. Karst, *J. Trace Elem. Med. Biol.* **2018**, *50*, 100.
- [66] K. Günther, A. Von Bohlen, C. Strompen, *Anal. Chim. Acta* **1995**, *309*, 327.
- [67] M. González, L. Tapia, M. Alvarado, J. D. Tornero, R. Fernández, *J. Anal. At. Spectrom* **1999**, *44*, 885.
- [68] R. Fernández-Ruiz, J. D. Tornero, V. M. González, C. A. Bedate, *Analyst* **1999**, *124*, 583.
- [69] Z. Majer, S. Bősze, I. Szabó, V. G. Mihucz, A. Gaál, G. Szilvágyi, G. Pepponi, F. Meirer, P. Wobrauschek, N. Szoboszlai, D. Ingerle, C. Strelí, *Microchem. J.* **2015**, *120*, 51.
- [70] D. Von Czarnowski, E. Denkhaus, K. Lemke, *Spectrochim. Acta Pt B.* **1997**, *52*, 1047.
- [71] L. Guangcheng, Y. Wu, H. Yuing, Z. Limin, *Guangpuxue Yu Guangpu Fenxi* **2000**, *20*(2), 240.
- [72] T. Magalhães, A. von Bohlen, M. L. Carvalho, M. Becker, *Spectrochim. Acta Pt B.* **2006**, *61*, 1185.
- [73] M. L. Carvalho, T. Magalhães, M. Becker, A. von Bohlen, *Spectrochim. Acta Pt B.* **2007**, *62*, 1004.
- [74] N. Szoboszlai, A. Réti, B. Budai, Z. Szabó, J. Kralovánszky, G. Záray, *Spectrochim. Acta, Pt B.* **2008**, *63*, 1480.
- [75] R. G. Leitão, A. Palumbo Jr., P. A. V. R. Souza, G. R. Pereira, C. G. L. Canellas, M. J. Anjosa, L. E. Nasciutti, R. T. Lopes, *Rad. Phys. Chem.* **2014**, *95*, 62.
- [76] M. Mages, M. Óvári, W. V. Tümping Jr., K. Kröpfl, *Anal. Bioanal. Chem.* **2004**, *378*, 1095.
- [77] S. Woelfl, M. Mages, S. Mercado, L. Villalobos, M. Óvári, F. Encina, *Anal. Bioanal. Chem.* **2004**, *378*, 1088.
- [78] G. Pepponi, P. Lazzeri, N. Coghe, M. Bersani, E. Gottardini, F. Cristofolini, G. Clauser, A. Torboli, *Spectrochim. Acta Pt B.* **2004**, *59*, 1205.
- [79] B. Markert, U. Reus, U. Herpin, *Sci. Total Environ.* **1994**, *152* (3), 213–220.
- [80] G. Zarazúa-Ortega, J. Poblano-Bata, S. Tejeda-Vega, P. Ávila-Pérez, C. Zepeda-Gómez, H. Ortiz-Oliveros, G. Macedo-Miranda. Assessment of Spatial Variability of Heavy Metals in Metropolitan Zone of Toluca Valley, Mexico, Using the Biomonitoring Technique in Mosses and TXRF Analysis. *The Scientific World Journal.* **2013**, *2013*, 1. <http://dx.doi.org/10.1155/2013/426492>.
- [81] M. Natali, A. Zanella, A. Rankovic, D. Banas, C. Cantaluppi, L. Abbadie, J.-C. Lata, *Environ. Sci. Pollut. Res.* **2016**, *23*, 23496.
- [82] F. R. Espinoza-Quifiones, A. N. Módenes, L. P. Thomé, S. M. Palácio, D. E. G. Trigueros, A. P. Oliveira, N. Szymanski, *Chem. Eng. J.* **2009**, *150*, 316.
- [83] R. Höhner, S. Tabatabaei, H.-H. Kunz, U. Fittschen, *Spectrochim. Acta Pt B.* **2016**, *125*, 159.
- [84] R. Fernández-Ruiz, M. Malki, A. Morato, I. Marin, *J. Anal. At. Spectrom* **2011**, *26*, 511.
- [85] J. Fiedor, B. Ostachowicz, M. Baster, M. Lankosza, K. Burda, *J. Anal. At. Spectrom* **2016**, *31*, 2078.
- [86] Q. A. Pankhurst, N. K. T. Thanh, S. K. Jones, J. Dobson, *J. Phys. D Appl. Phys.* **2009**, *42*, 224001.
- [87] R. Fernández-Ruiz, R. Costo, M. P. Morales, O. Bomati-Miguel, S. Veintemillas-Verdaguer, *Spectrochim. Acta Pt B.* **2008**, *63*, 1387.
- [88] F. J. Antosz, Y. Xiang, A. R. Diaz, A. J. Jensen, *J. Pharm. Biomed. Anal.* **2012**, *25*(62), 17.
- [89] R. Fernández-Ruiz, M. J. Redrejo, J. F. Eberhardt, M. Ramos, T. Fernández, *Anal. Chem.* **2014**, *86*, 7383.
- [90] G. Mankovskii, A. Pejović-Milić, *J. Anal. At. Spectrom* **2018**, *33*, 395.
- [91] S. I. Zheludeva, N. N. Novikova, O. V. Konovalov, M. V. Kovalchuk, N. D. Stepina, E. A. Yur'eva, I. V. Myagkov, Y. K. Godovski, N. N. Makarova, A. M. Rubtsov, O. D. Lopina, A. I. Erko, A. L. Tolstikhina, R. V. Gainutdinov, V. V. Lider, E. Y. Tereshchenko, L. G. Yanusova, *Crystallogr. Rep.* **2003**, *48*, S25–36.
- [92] S. I. Zheludeva, N. N. Novikova, O. V. Konovalov, M. V. Kovalchuk, N. D. Stepina, E. Y. Tereshchenko, *Mater. Sci. Eng. C* **2003**, *23*, 567.
- [93] M. Brücher, P. Jacob, A. von Bohlen, J. Franzke, C. Sternemann, M. Paulus, R. Hergenröder, *Langmuir* **2010**, *26* (2), 959.
- [94] R. A. Heller, Q. Sun, J. Hackler, J. Seelig, L. Seibert, A. Cherkezov, W. B. Minich, P. Seemann, J. Diegmann, M. Pilz, M. Bachmann, A. Ranjbar, A. Moghaddam, L. Schomburg, *Redox Biol.* **2021**, *38*, 101764.

**How to cite this article:** R. Fernández-Ruiz, *X-Ray Spectrom* **2021**, *1*. <https://doi.org/10.1002/xrs.3243>